Taylor & Francis
Taylor & Francis Group

Vehicle System Dynamics
International Journal of Vehicle Mechanics and Mobility

ISSN: 0042-3114 (Print) 1744-5159 (Online) Journal homepage: http://www.tandfonline.com/loi/nvsd20

Insights into vehicle trajectories at the handling limits: analysing open data from race car drivers

John C. Kegelman, Lene K. Harbott & J. Christian Gerdes

To cite this article: John C. Kegelman, Lene K. Harbott & J. Christian Gerdes (2017) Insights into vehicle trajectories at the handling limits: analysing open data from race car drivers, Vehicle System Dynamics, 55:2, 191-207, DOI: 10.1080/00423114.2016.1249893

To link to this article: http://dx.doi.org/10.1080/00423114.2016.1249893

Published online: 03 Nov 2016.

VEHICLE SYSTEM DYNAMICS, 2017
VOL. 55, NO. 2, 191–207
http://dx.doi.org/10.1080/00423114.2016.1249893

Insights into vehicle trajectories at the handling limits: analysing open data from race car drivers

John C. Kegelman, Lene K. Harbott and J. Christian Gerdes

Stanford University, Stanford, CA, USA

ABSTRACT

Race car drivers can offer insights into vehicle control during extreme manoeuvres; however, little data from race teams is publicly available for analysis. The Revs Program at Stanford has built a collection of vehicle dynamics data acquired from vintage race cars during live racing events with the intent of making this database publicly available for future analysis. This paper discusses the data acquisition, post-processing, and storage methods used to generate the database. An analysis of available data quantifies the repeatability of professional race car driver performance by examining the statistical dispersion of their driven paths. Certain map features, such as sections with high path curvature, consistently corresponded to local minima in path dispersion, quantifying the qualitative concept that drivers anchor their racing lines at specific locations around the track. A case study explores how two professional drivers employ distinct driving styles to achieve similar lap times, supporting the idea that driving at the limits allows a family of solutions in terms of paths and speed that can be adapted based on specific spatial, temporal, or other constraints and objectives.

ARTICLE HISTORY
Received 23 June 2016
Revised 16 September 2016
Accepted 9 October 2016

KEYWORDS
Vehicle dynamics; driver behaviour; driver–vehicle systems; trajectory modelling; sensors; database

1. Introduction

Race car drivers have the ability to safely control a vehicle at the limits of handling. As advanced driver assistance and autonomous driving systems continue to develop, race car drivers can offer insights into vehicle control during manoeuvres that require full handling capabilities. While racing teams collect and analyse data to improve performance, the motivation and analysis typically depend on the specific vehicle or driver and are not publicly available, but the overall driving behaviour is generally useful to anyone interested in vehicle dynamics and control at the limits of friction. Widespread access to data from professional race car drivers provides insight into how the best human drivers operate, and enables the design of vehicle safety systems that mimic their behaviour.

Large volumes have been dedicated to racing cars. While Milliken and Milliken's comprehensive 'Race car vehicle dynamics' [1] details the fundamental engineering concepts, researchers, race engineers, and enthusiasts alike can benefit from real-world applications and examples. Beginning with Taruffi in 1959 [2] and continuing with books by Bentley [3]

CONTACT John C. Kegelman kegelman@stanford.edu

and Krumm [4], authors have provided descriptions of how professional race car drivers approach racing. These texts include both qualitative and quantitative assessments of driver performance specific to racing, but do not focus on how these techniques can be more broadly applicable. Brown [5], Knox [6], and Segers [7] describe how to analyse data collected from race cars, but the analysis typically focuses on improving the performance of the vehicle or driver.

Several researchers have analysed or drawn inspiration from professional race car drivers for vehicle dynamics and control applications. Metz and Williams used a quasi-optimisation routine to compute steering, braking, and acceleration control inputs that minimised time through a single track section, and compared the results with performance data measured from three Formula One drivers [8]. Velenis et al. analysed a trail-braking manoeuvre through a 90° corner recorded from an expert rally driver. They generated similar steering, throttle, and braking commands by minimising time using numerical optimisation subject to specific boundary conditions [9]. Katzourakis et al. described an approach for instrumenting a vehicle for high-speed driving research, and provided a comparison between novice and expert driving behaviours for a single driving task [10]. Kritayakirana and Gerdes developed an autonomous controller inspired by professional race car driving techniques and implemented it on an Audi TTS [11,12].

Additionally, many have explored the idea of an ideal racing trajectory. As early as 1971, Roland and Thelin used computer simulation to optimise the Watkins Glen Grand Prix circuit by fitting a polynomial to the empirically determined 'racing groove' and solving a minimum-time problem [13]. Casanova developed a numerical optimisation programme to determine the theoretical optimal lap [14,15]. The sensitivity studies highlight the challenges involved in simulating highly complex, nonlinear vehicle models with many uncertain or changing parameters. Theodosis and Gerdes used a nonlinear gradient descent to optimise paths for an autonomous race car and compared the resulting paths to those driven by a professional race car driver [16]. Gerdts et al. implemented a moving horizon approach to find a locally optimal reference trajectory for an autonomous test car to eliminate the unpredictable influence of human drivers when evaluating vehicle setups [17]. Gerdts notes that even professional drivers produce large ranges of dispersion when driving at the limits though a given test-course; however, there is still much insight to be gained from studying the variability of racing trajectories.

In partnership with the Revs Institute for Automotive Research in Naples, Florida, the Revs Program at Stanford has built a database of race car vehicle dynamics data with the intent of making this information publicly available for further analysis. The objectives fit within the engineering and historical research goals of the Revs Program at Stanford by investigating how professional race car drivers control vehicles at the limits of handling while contributing to the characterisation and documentation of historically significant automobiles. By studying vintage race cars, as opposed to modern race cars, the insights gained can be applied more directly to production cars because the vehicle performance is not dominated by aerodynamic effects.

This paper introduces the Revs Vehicle Dynamics Database and examines trajectories driven by expert drivers while racing. Section 2 details the signals recorded, the sensors and data acquisition hardware, the venues, and the vehicles included in the database as of this writing. Section 3 quantifies the dispersion of paths driven during live vintage racing events and reveals highly repeatable paths at specific locations around a race track.

The paper concludes with a case study of two contrasting driving styles in Section 4, comparing different approaches to trade-offs between distance travelled, path curvature, and speed. We find that two highly skilled drivers achieved similar results, as measured by lap times, while exhibiting distinct driving styles, expressed by significantly different distances travelled around a race track. Section 4 also includes a discussion of how these trade-offs can be adjusted depending on the driving situation, providing insights into how a family of solutions can be used to drive at the limits of handling.

2. Data acquisition

2.1. Vehicle instrumentation

Unlike modern vehicles, the vintage race cars included in this study had few existing sensors. The automobiles are frequently on display and have inherent value as historical objects, so mounting the sensors had to be minimally invasive. The sensors were selected to enable a wide range of data analysis applications. Figure 1 gives an overview of the areas of interest. The sensor suite included more than 20 analog sensors, an inertial navigation system (INS), and video recordings from various viewing angles.

A major focus of the data collection was on the driver's actions to gain insights into professional race car driver behaviour. To accomplish this, sensors measured all driver inputs to the vehicle. Steering angle was measured with a string potentiometer by tracking the linear motion of the steering rack or wrapping around the steering column. As shown in Figure 2(a), throttle position was sensed with another string potentiometer affixed to the throttle linkage. The driver's brake and clutch inputs were measured with force-sensitive

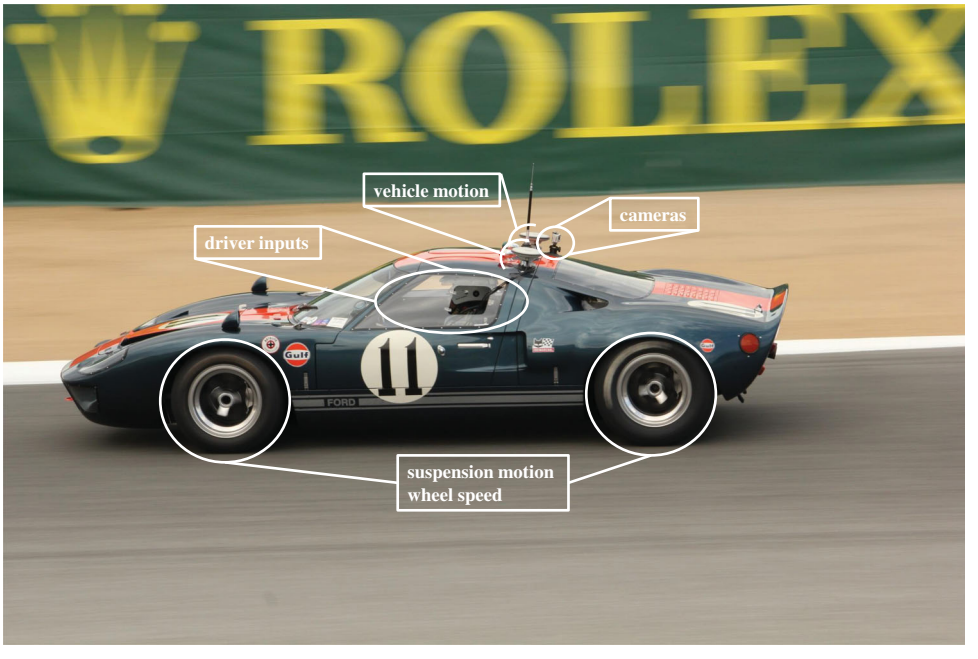

Figure 1. Overview of the data categories collected by the sensor suite.

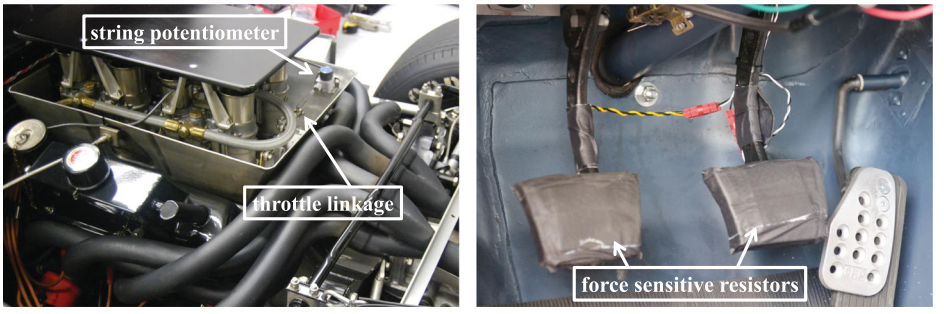

Figure 2. Sensors used to record driver inputs. (a) A string potentiometer mounted to existing bolt holes in the engine compartment supplied a high-resolution measurement of throttle position. (b) Force-sensitive resistors taped to each pedal provided safe and minimally invasive measurements of pedal engagement.

resistors taped to each pedal, as shown in Figure 2(b). These did not necessarily provide a precise indication of pedal force or fluid pressure but supplied a robust signal of pedal engagement. Engine speed was sensed with a universal speed measurement instrument by detecting pulses from either an inductive pickup on a single spark plug wire or a tachometer output wire of the ignition box. The engine speed, vehicle speed, and drivetrain gear ratios were then used to determine gear position.

Another priority was the vehicle motion captured by an INS aided by Global Navigation Satellite System (GNSS) signals. The system integrates an Inertial Measurement Unit (IMU) with survey-grade GNSS receivers to report the vehicle's real-time position, attitude, velocity, angular rate, and acceleration. The GNSS receivers utilised differential corrections either from OmniSTAR (resulting in decimeter-level position accuracy) or from a local reference station (resulting in centimeter-level position accuracy). Suction cups fixed either one or two GNSS antennas to the roof of each car, as shown in Figure 3(a). For the majority of the instrumented vehicles, the seat brackets provided suitable attachment points for the IMU enclosure once the passenger seat was removed, also shown in Figure 3(a) along with the data acquisition box.

Figure 3. Systems used to record vehicle motion and race context. (a) A GNSS-aided Inertial Navigation System recorded overall vehicle body motion. (b) Forward- and driver-facing cameras added indispensable situational context to the acquired data.

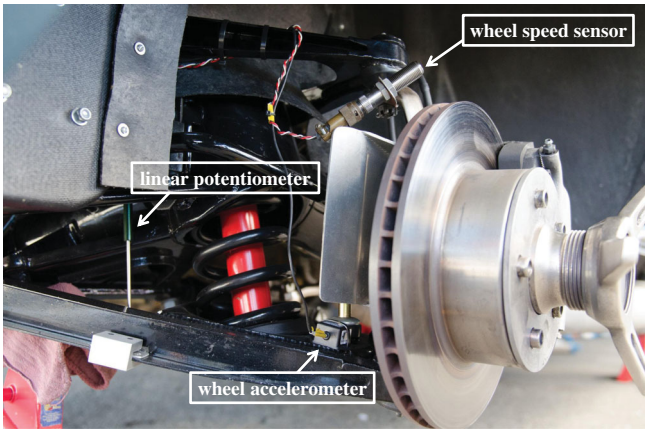

Figure 4. Sensors mounted in each wheel-well captured chassis and wheel motion.

To augment the vehicle data collected during testing, multiple cameras placed at specific viewing angles captured the entire racing experience, including the driver's behaviour and surroundings. This additional visual information provided context to the raw vehicle data. Typical views were forward-facing to capture the driver's visual area, driver-facing to capture the driver's behaviour (cameras shown in Figure 3(b)), and rear-facing to capture the behaviour of surrounding vehicles.

Four sensors at each corner of the car captured the wheel and suspension motion. A linear potentiometer mounted approximately parallel to a major suspension component, such as the spring or damper, measured suspension travel. This information characterises suspension elements and indicates when the suspension travel reaches its mechanical limits in both jounce and rebound. Two accelerometers, one mounted outboard of suspension elements as close to the wheel as possible and the other mounted to the vehicle structure inboard of suspension elements, measured vertical accelerations at the wheel and chassis, respectively. These measurements can validate quarter-car models that characterise the unsprung and sprung mass motion. A differential Hall effect sensor measured wheel rotation rate via different methods determined by packaging constraints. One method detected the presence of a magnet attached to the inside of the wheel rim and another sensed the passing of brake caliper bolt heads. Many of these sensors can be seen in Figure 4.

All vehicle signals were sampled and recorded with on-board MoTeC hardware. Two Synchronous Versatile Input Modules (SVIMs) sampled the analog signals and communicated them via Controller Area Network (CAN) to an Advanced Central Logger (ACL). The ACL also recorded CAN data from the INS and sent synchronisation pulses to the Video Capture System (VCS). Table 1 summarises the vehicle channels and their sample rates, which were chosen to capture the underlying system dynamics of interest.

2.2. Vehicles

The vehicles used in this study are owned by the Revs Institute for Automotive Research located in Naples, Florida. Table 2 shows the complete list of vehicles that have been instrumented. The remainder of this paper includes data from one of the vehicles, described below.

Table 1. Sampling rates for the vehicle data channels.

Channel	Sensor	Sample rate(Hz)
Position	INS	100
Velocity	INS	100
Acceleration	INS	100
Attitude	INS	100
Angular rate	INS	100
Engine speed	Tachometer	100
Steering angle	Potentiometer	500
Throttle position	Potentiometer	500
Brake	FSR	500
Clutch	FSR	500
Wheel acceleration	Accelerometer	1000
Chassis acceleration	Accelerometer	1000
Suspension travel	Potentiometer	1000
Wheel speed	Hall effect	100

Table 2. Specifications for each vehicle that has been instrumented to be included in the database.

Year	Make	Model	Displacement (cm^3)	Peak power(kW)	Wheel base(m)	Mass(kg)
1960	Porsche	Abarth-Carrera	1587	101 at 6500 rpm	2.10	799
1967	Porsche	910	1991	164 at 8000 rpm	2.30	599
1966	Ford	GT40	4736	291 at 7000 rpm	2.41	832
1963	Corvette	Grand Sport	6178	362 at 6000 rpm	2.49	975
1965	Ferrari	250 LM	3286	239 at 7500 rpm	2.40	850

2.2.1. 1963 Corvette Grand Sport.

Figure 5(a) shows the instrumented Corvette Grand Sport, serial number 004. The fourth of only five built, this lightweight version of the iconic Sting Ray saw limited racing action due to General Motors' ban on racing [18].

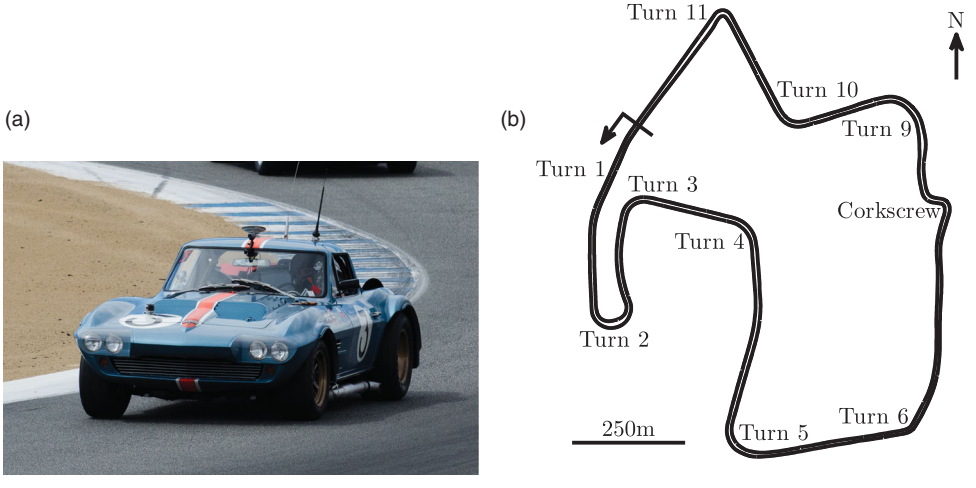

Figure 5. Data were collected from vehicles owned by the Revs Institute for Automotive Research during live vintage race events. (a) The 1963 Corvette Grand Sport negotiating Turn 3 at Laguna Seca during the Monterey Motorsports Reunion. (b) Laguna Seca in Monterey, California.

2.3. Venues and events

Two annual events served as the primary data collection venues: the Monterey Motorsports Reunion, held each August in Monterey, California; and Targa Sixty-Six, held each February in Jupiter, Florida. The Monterey Motorsports Reunion takes place at Laguna Seca, a 3.6 km track consisting of 11 turns and 55 m of elevation change, shown in Figure 5(b). Targa Sixty-Six is held at Palm Beach International Raceway, a 3.3 km track consisting of 10 turns and a 1 km straightaway.

2.4. Digital Preservation and Access

The Stanford Digital Repository (https://sdr.stanford.edu/) hosts the resulting multimedia collection, made available under the Open Data Commons Attribution License (ODC-By) [19], with items corresponding to each event. Each item includes comma-separated values (CSV) files containing vehicle data, one for each track session, and video files for up to four camera views per track session. The collection items also contain a text file with vehicle parameters including dimensions, mass distribution, and other metadata. Table 3 contains the persistent URL where each event currently included in the database is available.

3. Path repeatability

Analysing and optimising vehicle trajectories, specifically racing lines, is an extensive area of research [8,13,14,16,17,20–24]. The following section investigates the similarities of racing lines driven by professional race car drivers during live races using the data from the Revs Vehicle Dynamics Database.

This analysis includes data from two participants who drove the 1963 Corvette Grand Sport during the 2013 Monterey Motorsports Reunion at Laguna Seca. Over the course of the event, the drivers provided many examples of racing lines. The method described below quantifies the repeatability of the paths driven by each participant, and identifies specific points or sections of the track corresponding to low lateral path dispersion.

3.1. Statistical dispersion of driven paths

Participants 1 and 2 drove the vehicle during four separate race sessions each, completing a total of 29 and 30 laps, respectively. To preserve the focus on quantifying the performance of expert drivers at the handling limits, we sought to isolate data recorded under inapplicable conditions, such as when racing was suspended, while retaining as much data

Table 3. Persistent URLs corresponding to each event included in the Revs Vehicle Dynamics Database as of this writing.

Event	Persistent URL
2013 Targa Sixty-Six	http://purl.stanford.edu/yf219gg2055
2013 Monterey Motorsports Reunion	http://purl.stanford.edu/tt103jr6546
2014 Targa Sixty-Six	http://purl.stanford.edu/hd122pw0365

as possible representing the diverse circumstances experienced during real racing situations. Manually identifying contextually anomalous data instances can be time-intensive and subjective, so a generalised extreme Studentized deviate (ESD) many-outlier procedure [25] was implemented to detect outliers based on lap times. This procedure tested for up to eight outliers at a significance level of 5%. The generalised ESD procedure identified three lap times as outliers from Participant 1's data sets and none from Participant 2's. Further investigation revealed the three outlier laps to have been driven behind a safety car while the track was under caution and racing was suspended; therefore, these laps were removed from the analysis.

For each of the remaining laps, the driven path was mapped to the track centre line in terms of distance along the centre line s and lateral offset from the centre line e, as shown in Figure 6.

To evaluate the statistical dispersion of the driven lines, we chose the mean absolute deviation from the median (MAD median) as a robust measure of the distribution's scale [26]. The MAD median for each path was calculated as

$$\mathrm{MAD}\{e_i\} = \frac{1}{n}\sum_{j=1}^{n}\left\{\left|e_{i,j} - \underset{j\in[1,\ldots,n]}{\mathrm{median}}\{e_{i,j}\}\right|\right\}, \tag{1}$$

where $\mathrm{MAD}\{e_i\}$ is the mean absolute deviation from the median lateral offset e at each discrete point i for each lap j, and n is the total number of laps analysed per driver.

Figure 7 shows Participant 1's MAD median path versus distance (a) and projected onto the track map (b) from 26 laps in the 1963 Corvette Grand Sport around Laguna Seca. Figure 8 shows Participant 2's MAD median path versus distance (a) and projected onto the track map (b) from 30 laps driving the same vehicle at Laguna Seca.

Points 'A'–'I' in Figures 7 and 8 mark local minima in MAD median path and occur at similar track locations, indicating that the drivers exhibit highly repeatable behaviour at particular sections of the track. These locations approximately correspond to turns, or local maxima in path curvature, providing quantitative evidence to support the qualitative notion that drivers strive to hit the 'apex' of turns on each lap.

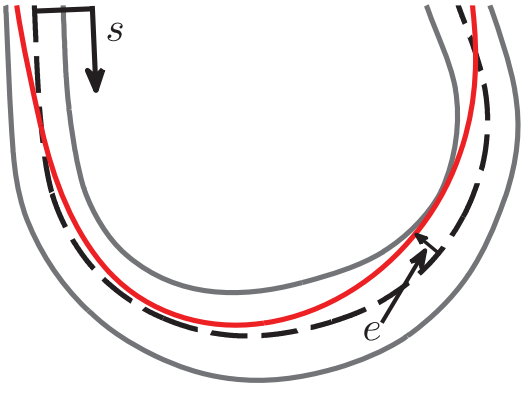

Figure 6. The path taken by the driver on each lap was mapped in terms of distance along the track centre line s and lateral offset from the track centre line e. The centre lines were discretised at evenly spaced 10 cm intervals.

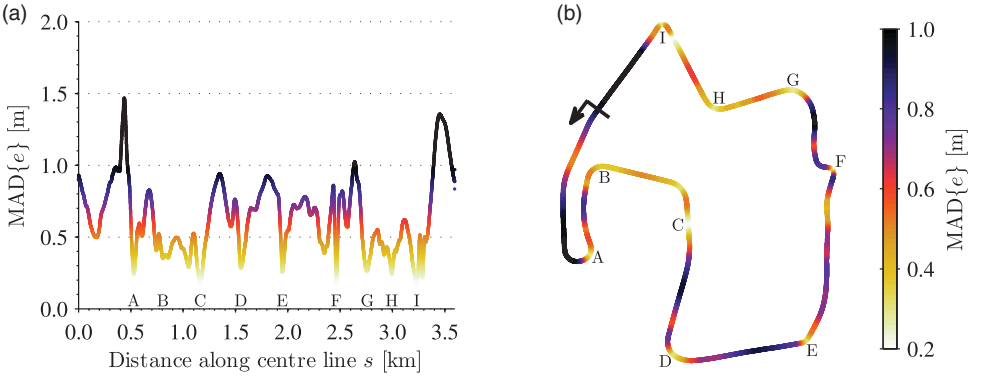

Figure 7. The paths driven by Participant 1 in the Corvette Grand Sport around Laguna Seca were highly similar at particular locations on the track. Participant 1's MAD median path versus distance (a) shows distinct local minima, marked 'A'–'I,' which correspond to turns in the track (b). (a) Participant 1, Corvette Grand Sport, $n_1 = 26$ laps around Laguna Seca. (b) Participant 1's MAD median path projected onto the track map. The arrow indicates the direction of travel.

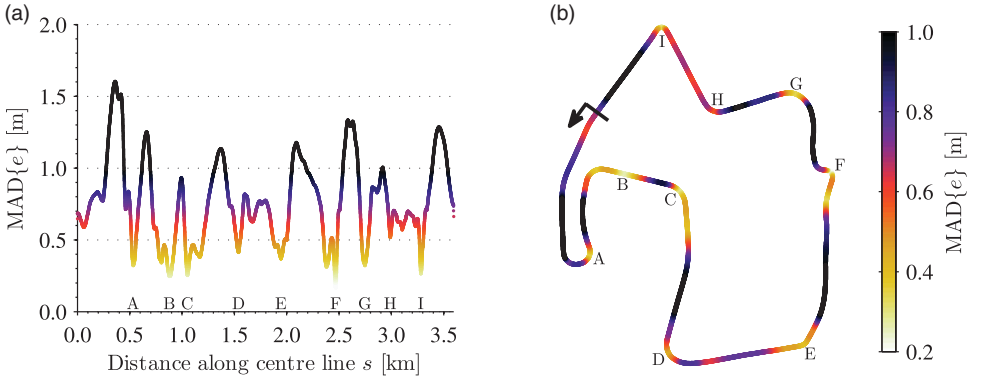

Figure 8. Consistent with the results from Participant 1, Participant 2's paths driven in the Corvette Grand Sport around Laguna Seca were highly similar at corresponding locations on the track. This suggests that the importance of these locations is common between drivers. (a) Participant 2, Corvette Grand Sport, $n_2 = 30$ laps around Laguna Seca. (b) Participant 2's MAD median path projected onto the track map. The arrow indicates the direction of travel.

To further illustrate this point, the curvature of the driven paths can be calculated as

$$\kappa = \frac{\mathrm{d}\psi}{\mathrm{d}s_p} = \frac{\mathrm{d}\psi}{\mathrm{d}t}\frac{\mathrm{d}t}{\mathrm{d}s_p}, \\ = \frac{\dot{\psi}}{U_H}, \tag{2}$$

where κ is the horizontal path curvature, ψ is the track angle or angle of the vehicle's velocity vector, s_p is the distance along the driven path, and U_H is the vehicle's horizontal speed.

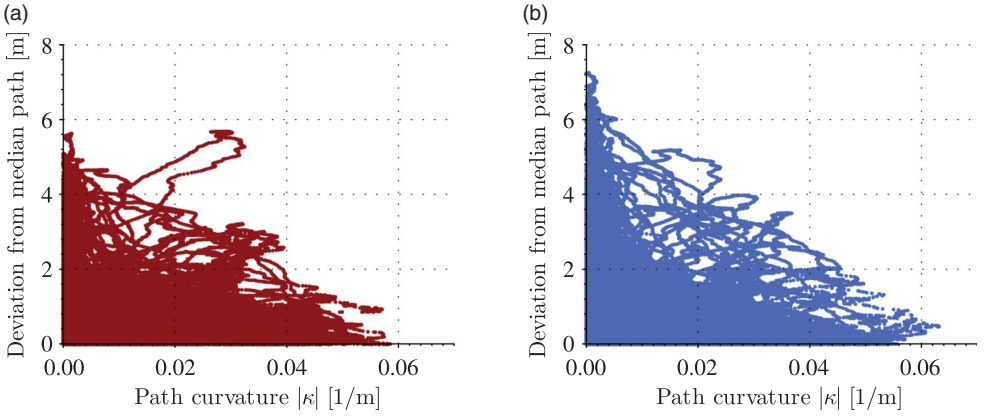

Figure 9. Drivers follow very similar paths each time through sections with high path curvature. High absolute path curvature, i.e. small turn radii, corresponds to low absolute deviation from the median racing lines driven by both Participant 1 (a) and Participant 2 (b) in the Corvette Grand Sport at Laguna Seca. (a) Participant 1, Corvette Grand Sport, $n_1 = 26$ laps around Laguna Seca. (b) Participant 2, Corvette Grand Sport, $n_2 = 30$ laps around Laguna Seca.

Figure 9 shows scatter plots of the absolute deviation from the median lateral offset versus the absolute path curvature of the racing lines driven by both participants. The highest values of path curvature, corresponding to the smallest turn radii, are associated with the lowest values of absolute deviation, indicating that the drivers followed very similar paths each time through the tightest turns.

This analysis offers quantitative evidence to support the qualitative notion that drivers anchor their racing lines at various points around the track and provides a framework for quantifying the repeatability of race car driver performance. The correlation between high values of absolute path curvature and low values of absolute deviation is present in paths driven by two different drivers in the same vehicle. The next section explores how these drivers employ distinct driving styles to achieve similar results.

4. Case study of trade-offs while at the limits

The following analysis provides evidence that driving at the limits of handling allows a family of solutions in terms of paths and speeds. The data support that these highly skilled human drivers drive at or near the physical limits of the vehicle, and as shown in Section 3 do so very repeatably, yet patterns emerge that suggest the two participants had statistically distinct driving styles that lead to similar results.

All of the statistics presented in this section result from Kruskal–Wallis tests by ranks, a non-parametric one-way analysis of variance [27]. Each lap was treated as an independent sample grouped by participant, resulting in $n_1 = 26$ laps from Participant 1 and $n_2 = 30$ laps from Participant 2. For each subsection below, the groups were assumed to have identically shaped and scaled distributions, therefore the null hypothesis was that the grouped samples were from distributions with equal medians, and the P values presented measure the significance of the χ^2 statistic. The confidence intervals for each median presented were calculated according to Olive [28].

4.1. Overall results

Summary statistics offer the first evidence of differing driving styles. Figure 10 shows box plots for lap times (a) and lap distances (b) driven by each driver. The median lap times were not found to be significantly different ($P = .77$), which is consistent with the considerable overlap of the distributions shown in Figure 10(a), suggesting the drivers achieved similar results regarding the objective of minimum lap times. However, Figure 10(b) shows significantly different medians for the distance travelled per lap ($P < .001$), suggesting the drivers followed comparably distinct, while individually consistent, paths around the track.

A method analogous to that described in Section 3.1 mapped the speed along each driven path to the distance along the centre line, which was then averaged across each lap for the two participants, with the results shown in Figure 11. While the overall shapes of the two profiles are similar, subtle differences around the local minima point to different strategies regarding the speed at which turns were driven. Local maxima in speed profile naturally divided the track into nine segments, marked and labelled in Figure 11, which were then used to calculate the time, distance travelled, maximum path curvature, and minimum speed for each segment of each driven lap. Performing a series of one-way ANOVA for the time through each segment revealed that the participants had different median segment times for three of the nine segments: Turn 5 ($P = .013$), Turn 9 ($P = .020$), and Turn 10 ($P < .001$), marked by coloured circles in Figure 11 with the colour corresponding to the participant with the lower median segment time. Interestingly, the drivers' speed profiles appear categorically different through the segment marked 'Turns 1&2,' yet the resulting segment times are very similar. The following analysis examines three track segments for insights into the drivers' choices when trading-off paths and speed.

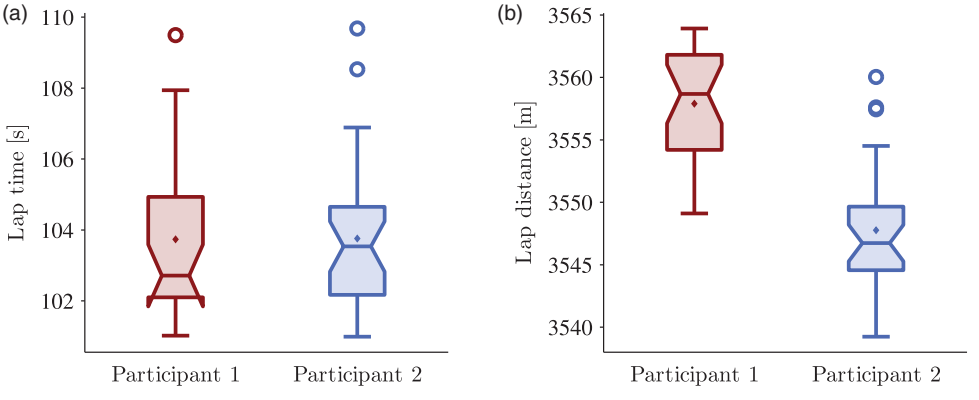

Figure 10. Box plots for lap time (a) and lap distance (b). On each box, the central line is the median, the point marked ◇ is the mean, the edges of the box are the 25th and 75th percentiles, the whiskers extend to the adjacent sample no further than 1.5 × IQR (interquartile range) beyond the edges, and possible 'outliers' are plotted individually. The notched sections provide visual comparison intervals and are calculated as median $\pm$ 1.57 × IQR/$\sqrt{n}$. (a) Considerable overlap in the distributions of lap times suggests the drivers achieved similar results. The mean and minimum times are nearly identical. (b) On average, Participant 2 travelled significantly less distance each lap ($P < .001$), suggesting each driver followed a distinct racing line.

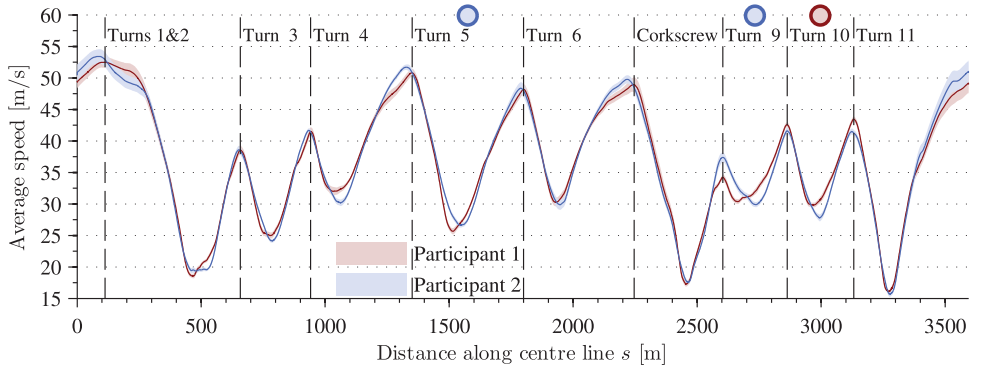

Figure 11. The different styles are apparent from the participants' average speed profiles, particularly around the local minima. The solid line is the average speed across all laps mapped to the track centre line, and the shaded area signifies a 95% confidence interval. The coloured ◯ indicate segments for which the median segment times were significantly different between participants ($P < .05$), with the colour corresponding to the participant with the lower median segment time.

4.2. Turn 2

Figure 12(a) shows Participant 1's median minimum speed was significantly lower than Participant 2's for 'Turn 2' ($P = .0050$), and the visualisation in Figure 12(b, c) shows that

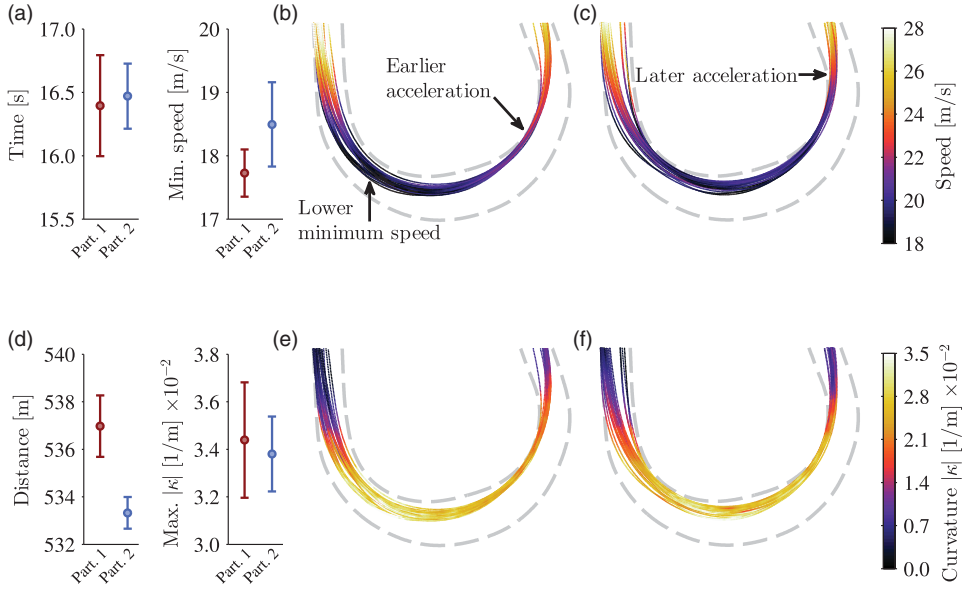

Figure 12. Turn 2. Participant 1 followed a 'slow-in, fast-out', or 'late-apex' approach while Participant 2's paths more closely resembled a 'diamond' or 'double-apex' approach. Participant 2 tended to travel shorter distances with higher minimum speeds; however, Participant 2's paths remained at relatively higher curvature for more of the turn while Participant 1 tended to accelerate earlier. The median segment times were largely similar. (a) Median segment time and minimum speed. (b) Participant 1: Speed. (c) Participant 2: Speed. (d) Median segment distance and maximum curvature. (e) Participant 1: Curvature. (f) Participant 2: Curvature.

the minimum speed tended to occur during the first part of the turn; however, Participant 1 tended to accelerate earlier through the latter part of the turn. The earlier acceleration coincided with paths of lower curvature through the latter part of the turn, as evidenced by Figure 12(e, f). This suggests Participant 1 followed a 'slow-in, fast-out' or 'late-apex' approach while Participant 2's paths more closely resembled a 'diamond' or 'double-apex' approach. Even though Participant 2's median distance travelled was significantly shorter ($P < .001$) and median minimum speed was significantly higher, the resulting segment times were largely similar due to the difference in speeds attained through the latter part of the turn.

4.3. Turn 9

Similar to 'Turn 2' and clearly shown in Figure 13(d), Participant 1 tended to travel a longer distance through 'Turn 9' ($P < .001$); however, unlike 'Turn 2,' Participant 2's median segment time was less than Participant 1's ($P = .020$). While the median minimum speeds were similar, Participant 1's minimum speeds tended to occur earlier in the turn, as shown in Figure 13(b, c), again suggesting a 'slow-in, fast-out' approach. Participant 2's shorter distance paths remained closer to the inside track boundary and realised a higher median maximum curvature ($P < .001$), but here resulted in a slight time advantage.

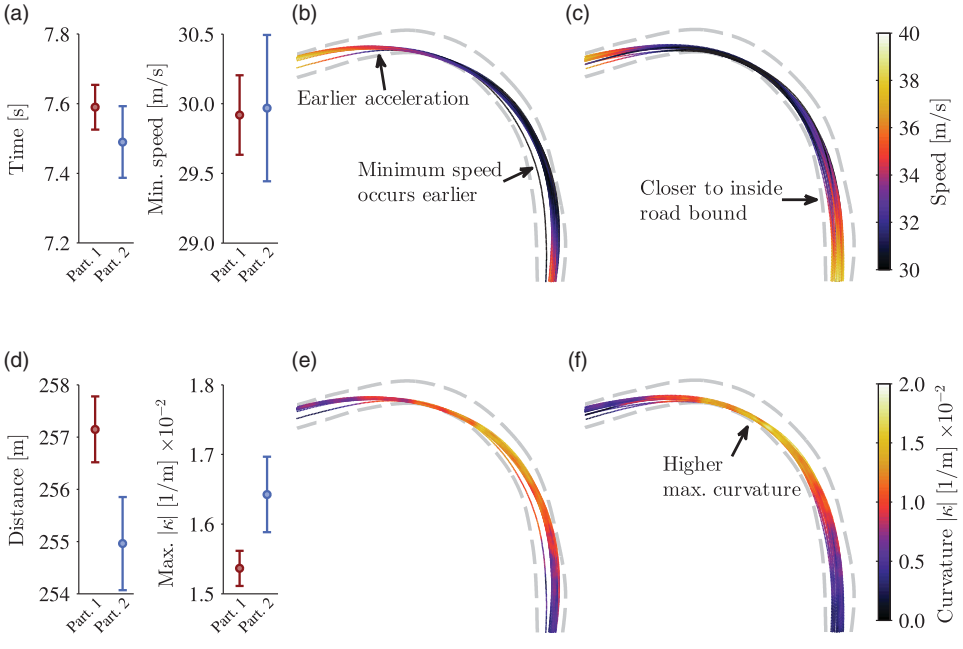

Figure 13. Turn 9. Similar to Turn 2, Participant 1 tended to follow a 'slow-in, fast-out' approach and travel longer distances, but in this case Participant 2's median segment time was faster ($P = .020$). (a) Median segment time and minimum speed. (b) Participant 1: Speed. (c) Participant 2: Speed. (d) Median segment distance and maximum curvature. (e) Participant 1: Curvature. (f) Participant 2: Curvature.

4.4. Turn 10

Figure 14 shows that Participant 2's paths through 'Turn 10' had a shorter median distance ($P < .001$) and tended to remain closer to the inside track boundary, similar to 'Turn 9.' In contrast, Participant 1's longer paths of lower maximum curvature ($P < .001$) afforded a higher median minimum speed ($P < .001$), ultimately leading to a lower median segment time ($P < .001$). Also, as indicated by the points marked 'H' in Figures 7 and 8 and apparent when comparing Figure 14(b, e) to Figure 14(c, f), Participant 2's paths had relatively more lateral dispersion through this segment.

Combining Turns '9' and '10' into a single analysis segment further accentuates the different driving styles, similar results, and the drivers' ability to connect consecutive track sections. When considered together, the median times for the combined segment were not found to be significantly different ($P = .34$). The time advantage gained by Participant 2 in 'Turn 9' is effectively negated by the time advantage gained by Participant 1 in 'Turn 10.' Participant 2 on average traverses a significantly shorter distance through the combined segment ($P < .001$); however, Participant 1's trade-offs in 'Turn 9' lead to a higher average speed at the transition between turns, as seen in Figure 11, and ultimately result in largely similar combined segment times.

4.5. Passing manoeuvre as change in objectives

To extend this framework beyond illuminating multiple ways to achieve similar segment times, a passing manoeuvre can illustrate how highly skilled human drivers adjust to changes in the surrounding environment. Figure 15 highlights such a passing scenario

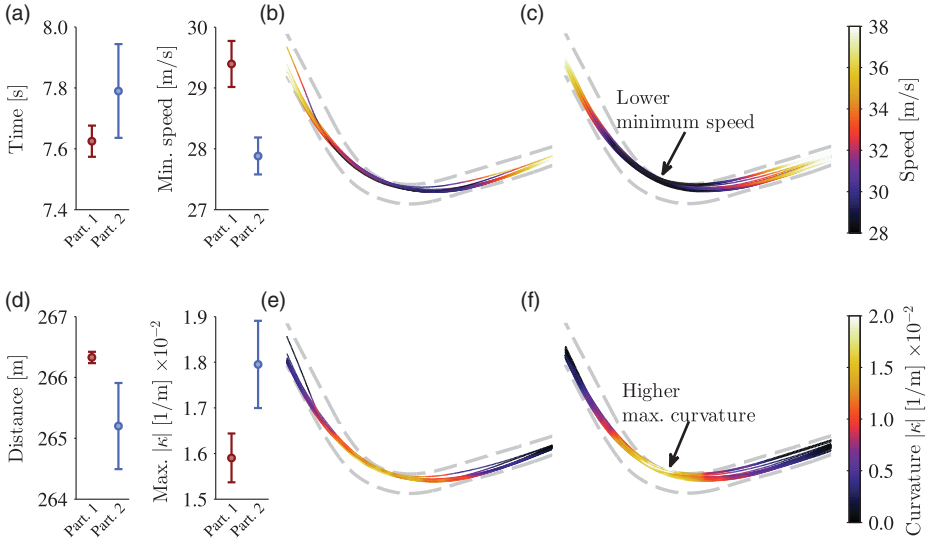

Figure 14. Turn 10. Consistent with the other segments examined, Participant 1's median distance travelled is longer; however, the lower curvature paths with higher minimum speeds resulted in a faster median segment time ($P < .001$). (a) Median segment time and minimum speed. (b) Participant 1: Speed. (c) Participant 2: Speed. (d) Median segment distance and maximum curvature. (e) Participant 1: Curvature. (f) Participant 2: Curvature.

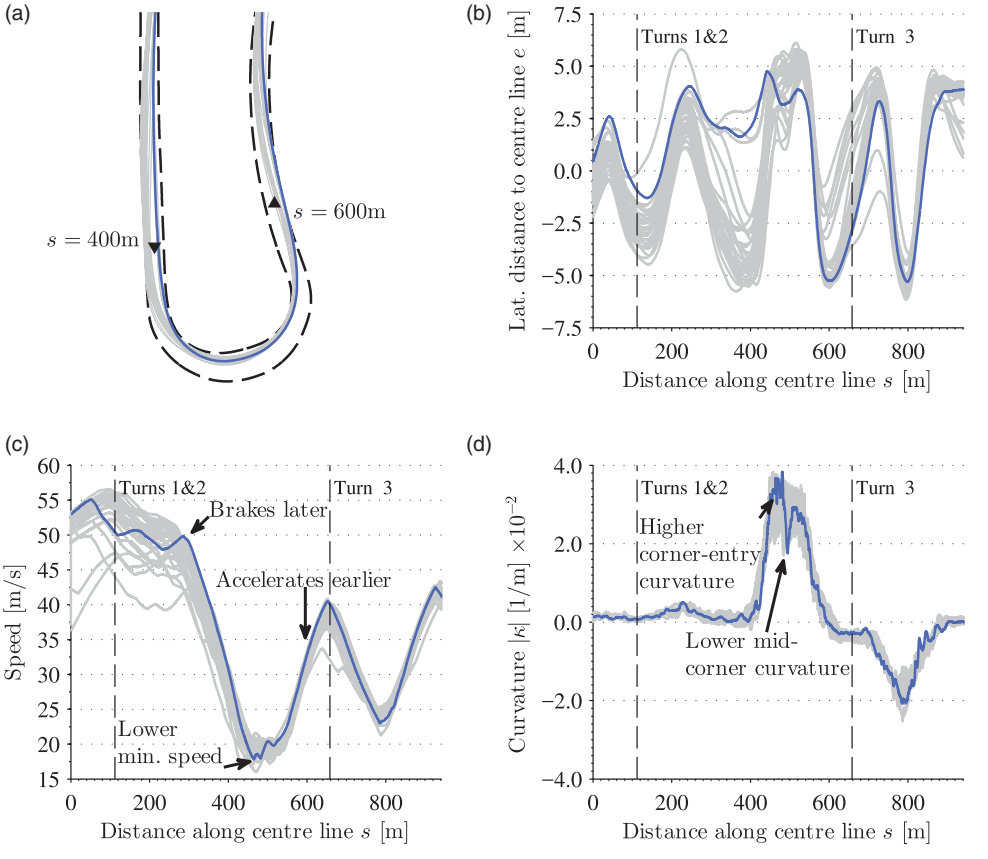

Figure 15. Relevant data traces from a passing manoeuvre completed by Participant 2 through Turn 2 at Laguna Seca. The driver adjusts the path and speed at which the turn is negotiated to accomplish the objective of overtaking a competing vehicle. (a) Turn 2 at Laguna Seca with the inside passing manoeuvre highlighted. This corner-exit coincides with a local minimum in MAD median path. (b) The highlighted trace shows a distinctly different lateral offset through the first part of the turn before returning to the nominal distribution. (c) Participant 2 braked later to initiate the pass but the inside path necessitated a lower minimum speed. (d) The resulting path shows local extrema in path curvature that are tightly coupled to the speed profile.

from Participant 2's data. As shown in Figure 15(a, b) and evidenced in the accompanying video, Participant 2 follows an inside line to overtake a relatively competitive vehicle. Figure 15(c) indicates Participant 2 began to decelerate later and slowed to a lower minimum speed during the first part of the turn to accommodate the higher path curvature, as seen in Figure 15(d). The subsequent lower mid-corner path curvature allowed Participant 2 to accelerate earlier, complete the manoeuvre, and return to his nominal path and speed profile. One way to frame this series of adjustments is that the primary objective of completing the segment as quickly as possible changed to passing the other vehicle by the end of the segment. In this case, the other vehicle represented a change in the spacial and temporal constraints or boundaries similar to the effects of a dynamic obstacle in real-world driving applications.

In summary, two expert drivers demonstrated different driving styles in the same vehicle under diverse racing conditions, yet achieved similar results. Participant 1 exhibited a 'slow-in, fast-out' approach and tended to travel longer distances through several track segments, while Participant 2 tended toward shorter distance, higher curvature paths, suggesting each made different trade-offs between paths and speed to achieve similar lap times. A passing manoeuvre executed by Participant 2 shows how these same trade-offs can be adjusted to achieve alternative objectives, depending on the current situation.

5. Conclusion

This paper introduces the Revs Vehicle Dynamics Database, and details the methods used for data acquisition, post-processing, and storage. The publicly available database includes data from a variety of vintage race cars, offering a rich resource for numerous interesting applications. An analysis of data currently available quantified the repeatability of paths driven by professional race car drivers during live race events, and showed that drivers exhibit highly repeatable paths at specific points around the track. A case study of the trade-offs between paths and speed revealed distinct driving styles that achieved similar results; significantly different distances travelled and speeds attained resulted in largely similar segment and overall lap times. A passing manoeuvre discussed in the context of a dynamic obstacle further illustrated that the trade-offs can be adjusted to achieve altered objectives while still operating the vehicle at the limits of handling.

Open access to data from expert drivers under real racing conditions facilitates the analysis of vehicle control under extreme operating conditions. This will inspire further development and validation of systems with the ability to fully utilise a vehicle's handling capabilities to keep its occupants safe.

Acknowledgments

The authors would like to thank Mr Miles Collier and the Revs Institute for Automotive Research, in particular Scott George, Bill Blume, and Mike Ellis, for their generous support of the Revs Program at Stanford. Furthermore, Jon Goh, Vincent Laurense, Jackie Liao, Shannon McClintock, Sara Rood, Will Tucker, and Scott Woods were instrumental in the hardware development and track support during the race events. The authors would also like to thank Mazda Raceway Laguna Seca and Palm Beach International Raceway for facilitating our testing, NovAtel and Oxford Technical Solutions for their GNSS and INS expertise, OmniSTAR for providing differential GPS corrections, and MoTeC for their instrumentation and data acquisition resources. And finally, the support from the members of the Dynamic Design Lab at Stanford University is always greatly appreciated.

Disclosure statement

No potential conflict of interest was reported by the authors.

ORCID

John C. Kegelman http://orcid.org/0000-0002-5490-9688

References

[1] Milliken WF, Milliken DL. Race car vehicle dynamics. Warrendale, PA: Society of Automotive Engineers; 1995.

[2] Taruffi P. The technique of motor racing. Cambridge, MA: Bentley; 1959.
[3] Bentley R. Ultimate speed secrets: the complete guide to high-performance and race driving. Minneapolis, MN: Motorbooks; 2011.
[4] Krumm M. Driving on the edge. Malvern, Worcestershire: Icon; 2011.
[5] Brown C. Making sense of squiggly lines. Huntington Beach, CA: CB-Racing; 2011.
[6] Knox B. A practical guide to race car data analysis. CreateSpace Independent Publishing Platform; 2011.
[7] Segers J. Analysis techniques for racecar data acquisition. Warrendale, PA: Society of Automotive Engineers; 2014.
[8] Metz D, Williams D. Near time-optimal control of racing vehicles. Automatica. 1989;25(6): 841–857.
[9] Velenis E, Tsiotras P, Lu J. Optimality properties and driver input parameterization for trail-braking cornering. Eur J Control. 2008;14(4):308–320.
[10] Katzourakis DI, Velenis E, Abbink D, et al. Race-car instrumentation for driving behavior studies. IEEE Trans Instrum Meas. 2012;61(2):462–474.
[11] Kritayakirana K, Gerdes JC. Autonomous vehicle control at the limits of handling. Int J Veh Autonom Syst. 2012;10(4):271–296.
[12] Funke J, Theodosis PA, Hindiyeh RY, et al. Up to the limits: autonomous Audi TTS. IEEE Intelligent Vehicles Symposium; 2012 Jun. p. 541–547. Available from: http://ieeexplore.ieee.org/lpdocs/epic03/wrapper.htm?arnumber=6232212
[13] Roland RD Jr, Thelin CF. Computer simulation of Watkins Glen grand prix circuit performance. Buffalo, New York: Cornell Aeronautical Laboratory; 1971 (Report No.: ZL-5002-K-1).
[14] Casanova D. On minimum time vehicle manoeuvring: the theoretical optimal lap [dissertation]. Cranfield University; 2000. Available from: http://hdl.handle.net/1826/1091.
[15] Casanova D, Sharp RS, Symonds P. Minimum time manoeuvring: the significance of yaw inertia. Veh Syst Dyn Int J Veh Mech Mob. 2000;34(2):77–115.
[16] Theodosis PA, Gerdes JC. Nonlinear optimization of a racing line for an autonomous racecar using professional driving techniques. ASME Dynamic Systems and Control Conference, Ft. Lauderdale, FL; 2012 Oct. p. 235–241.
[17] Gerdts M, Karrenberg S, Müller-Beßler B, et al. Generating locally optimal trajectories for an automatically driven car. Optim Eng. 2009;10(4):439–463.
[18] The Revs Institute for Automotive Research. 1963 Chevrolet Corvette Grand Sport; 2015. Available from: http://revsinstitute.org/the-collection/1963-chevrolet-corvette-grand-sport/
[19] Open Data Commons Attribution License; 2016. Available from: http://opendatacommons.org/licenses/by/1.0/
[20] Kelly DP, Sharp RS. Time-optimal control of the race car: a numerical method to emulate the ideal driver. Veh Syst Dyn Int J Veh Mech Mob. 2010;48(12):1461–1474.
[21] Perantoni G, Limebeer DJ. Optimal control for a Formula One car with variable parameters. Veh Syst Dyn Int J Veh Mech Mob. 2014;52(5):653–678.
[22] Tavernini D, Massaro M, Velenis E, et al. Minimum time cornering: the effect of road surface and car transmission layout. Veh Syst Dyn Int J Veh Mech Mob. 2013;51(10):1533–1547.
[23] Timings JP, Cole DJ. Minimum maneuver time calculation using convex optimization. J Dyn Syst Meas Control. 2013;135(3):1–9.
[24] Velenis E, Tsiotras P. Minimum time vs maximum exit velocity path optimization during cornering. IEEE International Symposium on Industrial Electronics, Dubrovnik, Croatia. Vol. I; 2005. p. 355–360.
[25] Rosner B. Percentage points for a generalized ESD many-outlier procedure. Technometrics. 1983;25(2):165–172.
[26] Habib EAE. Mean absolute deviation about median as a tool of explanatory data analysis. Int J Res Rev Appl Sci. 2012;11(3):517–523.
[27] Kruskal WH, Wallis WA. Use of ranks in one-criterion variance analysis. J Amer Statist Assoc. 1952;47(260):583–621.
[28] Olive DJ. A simple confidence interval for the median; 2005. Available from: http://lagrange.math.siu.edu/Olive/ppmedci.pdf